ELSEVIER

Neutron star cooling

D.G. Yakovlev[a], O.Y. Gnedin[b], M.E. Gusakov[a], A.D. Kaminker[a], K.P. Levenfish[a], and A.Y. Potekhin[a]

[a]Ioffe Physico-Technical Institute, Politekhnicheskaya 26, 194021 St. Petersburg, Russia

[b]Ohio State University, 760 1/2 Park Street, Columbus, OH 43215, USA

The impact of nuclear physics theories on cooling of isolated neutron stars is analyzed. Physical properties of neutron star matter important for cooling are reviewed such as composition, the equation of state, superfluidity of various baryon species, neutrino emission mechanisms. Theoretical results are compared with observations of thermal radiation from neutron stars. Current constraints on theoretical models of dense matter, derived from such a comparison, are formulated.

1. INTRODUCTION

Our knowledge of neutron star (NS) interiors is currently uncertain. In particular, the fundamental problem of the equation of state (EOS) at supranuclear densities in NS cores is still unsolved. Microscopic theories of dense matter are model dependent and give a large scatter of possible EOSs (e.g., Ref. [1]), from stiff to soft ones, with different compositions of inner NS cores (nucleons, hyperons, pion or kaon condensates, quarks). Thermal evolution of NSs depends on a model of dense matter which enables one to constrain the fundamental properties of dense matter by comparing simulations of NS cooling with observations.

NSs are born hot in supernova explosions, with the internal temperature $T \sim 10^{11}$ K. In about one minute after the birth a star becomes transparent for neutrinos generated in its interiors. In the following neutrino-transparent stage the star cools via neutrino emission from the entire stellar body and via heat transport through the envelope to the surface and subsequent thermal surface emission of photons. In a hundred of years the NS crust and core become thermally adjust and the NS interior becomes isothermal (with the only temperature gradient located near the surface). After that the effective surface temperature, T_s, reflects the thermal state of the core.

The recent development of the theory has been reviewed, e.g., in Refs. [2,3]. Here, we outline the current status of the problem.

2. OBSERVATIONS

Observations of isolated NSs, whose thermal surface radiation has been detected or constrained, are summarized in Fig. 1 (following Ref. [4]). We present the estimated NS ages t and effective surface temperatures T_s^∞ (as detected by a distant observer).
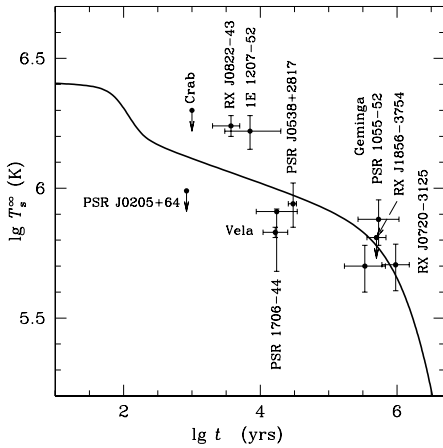
Figure 1. Observational limits of surface temperatures for several isolated NSs compared with the basic theoretical cooling curve of a non-superfluid NS model.
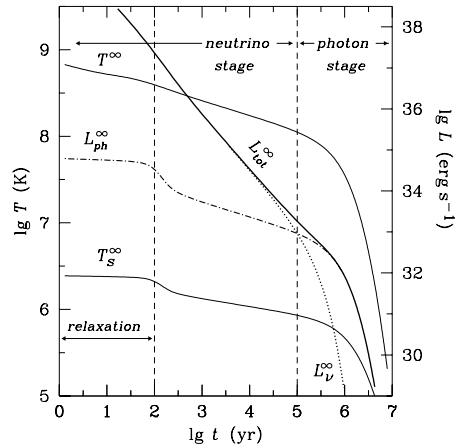
Figure 2. Internal and surface temperatures; neutrino, photon and total luminosities (redshifted for a distant observer) for the same NS model as in Fig. 1.

For the two youngest sources only upper limits on the surface temperature T_s^∞ have been established [5,6]. The surface temperatures of the next five sources, with ages $10^3 \lesssim t \lesssim 10^5$ years, have been obtained [7–11] by fitting their thermal radiation spectra with hydrogen atmosphere models. Such models are more consistent with other information on these sources (e.g., Ref. [12]) than the blackbody model. On the contrary, for Geminga and PSR B1055−52 we present the values of T_s^∞ [11,12] inferred using the blackbody spectrum because this spectrum is more consistent for these sources. The surface temperature of RX J1856.4−3754 is still uncertain. Following [4] we adopt the upper limit $T_s^\infty < 0.65$ MK. Finally, T_s^∞ for RX J0720.4−3125 is taken from Ref. [13], where the observed spectrum is interpreted with a model of a hydrogen atmosphere of finite depth.

As seen from Fig. 1, observational limits scatter in the $T_s^\infty - t$ plane. What can be learnt on dense matter in NS interiors from this scatter?

3. THEORY VERSUS OBSERVATIONS

A neutron star consists of a thin crust (of mass $\lesssim 10^{-2} M_\odot$, where $M_\odot$ is the solar mass) and a core (e.g., Ref. [1]). The core-crust interface is placed at the mass density $\rho \sim \rho_0/2$, where $\rho_0 \approx 2.8 \times 10^{14}$ g cm^{-3} is the density of saturated nuclear matter. The crustal matter contains atomic nuclei, electrons, and (at $\rho \gtrsim 4 \times 10^{11}$ g cm^{-3}) free neutrons. The core is further subdivided into the outer ($\rho \lesssim 2\rho_0$) and inner parts. The outer core consists of neutrons, with an admixture of protons, electrons, and muons. The composition of the inner core is still unknown. It may be the same composition as the outer core but may also contain hyperons, pion or kaon condensates, quark matter, or a
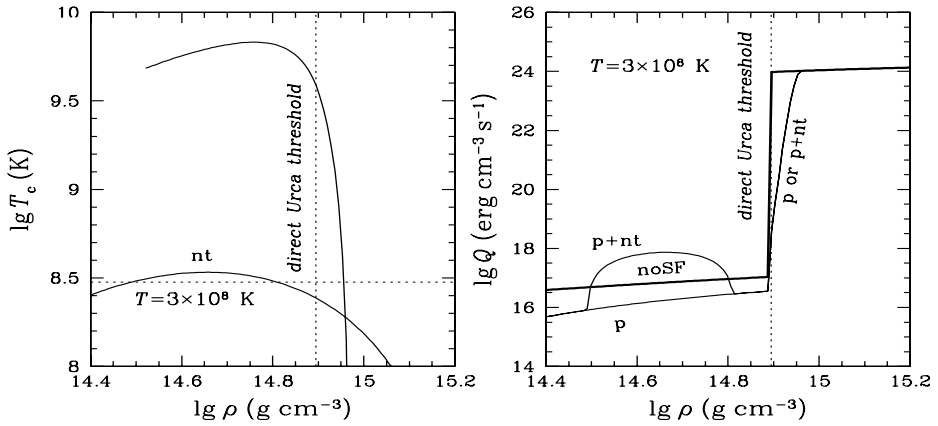
Figure 3. *Left:* Illustrative models of critical temperatures for proton (p) and neutron (nt) pairing in NS core. *Right:* Neutrino emissivity in the same NS core at the temperature $T = 3 \times 10^8$ K for non-superfluid matter (thick line; noSF) and in the presence of either proton pairing (p) or proton and neutron pairing (p+nt). The vertical dotted line indicates the threshold of the direct Urca process.

mixture of different phases.

NS matter is strongly degenerate. The EOS, NS masses M and radii are almost temperature independent. Low-mass NSs ($M \sim M_\odot$) have rather low central densities $\rho_c \lesssim 2\,\rho_0$ and do not possess inner cores. NSs with masses close to the maximum allowable mass ($M_{\max} \sim (1.5 - 2.5)\,M_\odot$, for different model EOSs) have massive inner cores.

NS cooling is calculated with a cooling code (e.g., Ref. [14]) in the form of *cooling curves*, $T_s^\infty(t)$ (e.g., Fig. 1). The initial cooling stage, $t \lesssim 100$ years, is accompanied by thermal relaxation of NS interiors (Fig. 2). As long as $t \lesssim 10^5$ years, a star cools mainly via neutrino emission from its interiors (mainly from the core); this is the *neutrino cooling stage*. Later, at $t \gtrsim 10^5$ years, the neutrino emission becomes inefficient, and the star cools via thermal surface emission of photons (the *photon cooling stage*).

NSs may have different masses, surface magnetic fields, composition of surface layers, etc., but they are supposed to have the same EOS and superfluid properties of internal layers. In the absence of exact microscopic theory of NS matter we will use several model EOSs and phenomenological superfluidity models.

The main regulators of NS cooling are:

(*a*) EOS and composition of NS cores which affect neutrino emission mechanisms;

(*b*) Superfluidity of baryons in NSs — it affects neutrino emission and heat content;

(*c*) The presence of light elements (accreted envelopes) and strong magnetic fields in NS surface layers. These factors affect the thermal conductivity and the relation between the internal and surface temperatures of the star.

We discuss these regulators below (except for magnetic fields whose effects are examined

in [15]). Other regulators are reviewed, e.g., in Ref. [2].

Figure 1 shows the *basic cooling curve*. It is calculated for a star with a non-superfluid nucleon core, where the powerful direct Urca process of neutrino emission is forbidden. Such a star cools mainly via neutrino emission produced by the less powerful modified Urca process; the accretion envelope is absent. This *basic curve* is *universal*, being almost independent of the EOS and NS mass. It cannot explain all the observations – some NSs are hotter and some colder than predicted by the curve. However, one can explain the data by employing other cooling regulators.

The effects of superfluidity and the direct Urca process, are demonstrated in Fig. 3. Here we adopt a moderately stiff EOS of dense nucleon matter suggested in Ref. [16] (the same version as used in [2]). This EOS opens the direct Urca process at $\rho > \rho_D = 7.851 \times 10^{14}$ g cm^{-3}, i.e., at $M > M_D = 1.358\,M_\odot$ (M being the gravitational mass) and gives NS models with $M_{\max} = 1.977\,M_\odot$. In non-superfluid matter the direct Urca process switches on sharply at $\rho > \rho_D$. However, neutrons and protons (like other baryons) in NS cores can be in superfluid state. As a rule, neutrons undergo triplet-state pairing, whereas protons undergo singlet-state pairing (e.g., Ref. [17]) with density dependent critical temperatures $T_{\mathrm{cnt}}(\rho)$ and $T_{\mathrm{cp}}(\rho)$ which are extremely sensitive to theoretical models. Superfluidity suppresses traditional neutrino emission mechanisms (the modified and direct Urca processes and nucleon-nucleon bremsstrahlung) but opens a new neutrino process associated with Cooper pairing of baryons [18]. Figure 3 shows some phenomenological $T_{\mathrm{cnt}}(\rho)$ and $T_{\mathrm{cp}}(\rho)$ curves (from Ref. [2]) and demonstrates that the direct Urca process and superfluidity greatly affect the neutrino emission (and, hence, NS cooling, as discussed later).

The cooling can be strongly different for low mass, medium mass, and high mass NSs.

3.1. Cooling of low-mass stars

Low-mass NSs possess only outer nucleon cores. Some cooling curves are presented in Fig. 4 for NS models constructed with the same EOS as in Fig. 3.

The solid curves are calculated assuming strong proton superfluidity p. It suppresses the modified Urca process in a low-mass NS. The neutrino luminosity of the star becomes lower (Fig. 3), being determined by a weaker mechanism of neutrino emission (neutron-neutron bremsstrahlung, unaffected by superfluidity as long as neutrons are non-superfluid). This rises the cooling curves at the neutrino cooling stage. The thick solid curve is calculated for a star without any accreted envelope. This curve (contrary to the basic curve in Fig. 1) goes high enough to explain the sources hottest for their age (RX J0822–43, 1E 1207–52, PSR B1055–52). Thus, we may treat these sources as low-mass NSs. The thin solid curve is calculated assuming, additionally, the presence of hydrogen or helium accreted envelope of mass $\Delta M = 10^{-8}\,M_\odot$. Light elements increase the thermal conductivity of the surface layers which further rises T_s^∞ at the neutrino cooling stage. The thin solid curve is close to the highest cooling curve provided by the standard cooling theory of NSs.

Actually, we do not need very strong proton superfluidity (such as model p) to interpret the observations. The dashed lines in Fig. 4 are the same as the solid lines, but the proton critical temperature $T_{\mathrm{cp}}(\rho)$ is reduced by a factor of 6. Weaker proton superfluidity relaxes the superfluid suppression of the modified Urca processes and lowers the cooling curves (with respect to the solid ones). Nevertheless, such superfluidity is still sufficient to interpret the observations: old hot sources are consistent with the thick dashed line (no
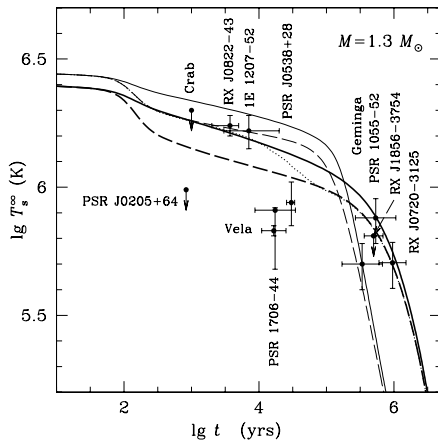
Figure 4. Cooling curves for the star with $M = 1.3\,M_\odot$ and nucleon core compared with the observations (see text for other explanations).
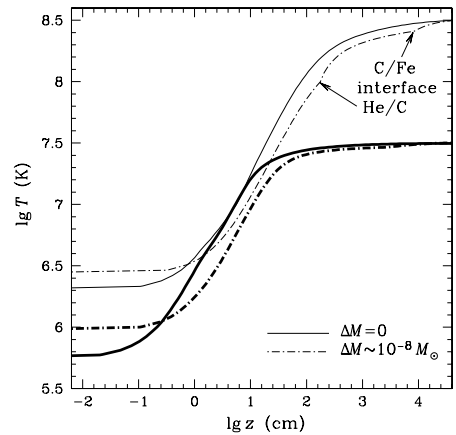
Figure 5. Temperature versus depth z in the NS envelope for two internal temperatures: $10^{8.5}$ K (light curves) and $10^{7.5}$ K (heavy curves), for nonaccreted and accreted envelopes.

accretion envelope) while young hot sources are well explained assuming an accreted envelope (thin dashed line). Finally, the dotted curve is the same as the thin dashed curve but the mass of the accreted envelope is assumed to decrease with time (e.g., due to diffuse burning [19]) as $\Delta M(t) = \Delta M(0) \exp(-t/\tau)$, with $\tau = 4000$ years. This model can also explain the observations of NSs hottest for their ages.

The effect of light-element envelopes on the cooling can be understood from Fig. 5. It shows the growth of temperature within the NS of mass $M = 1.4\,M_\odot$ and radius $R = 10$ km. The solid lines refer to a non-accreted (Fe) surface. The dot-and-dashed lines are for the thickest accreted (He and C) envelope that can survive with respect to nuclear burning. Because He and C have higher thermal conductivity than Fe, their presence makes the NS envelope more heat-transparent, increasing T_s.

3.2. Cooling of high-mass neutron stars

High-mass NSs have large central densities, masses $M \sim M_{\max}$, and contain massive inner cores. Microscopic theories predict that, as a rule, superfluidity dies out (and does not suppress neutrino emission) in the central parts of such stars.

One can propose very different cooling scenarios of high-mass NSs. The simplest scenario assumes non-superfluid nucleon cores where the direct Urca process is forbidden. The corresponding cooling curves would be the same as the basic curve in Fig. 1; they cannot explain all the observations.

It is widely thought that the neutrino emission in high-mass NSs is *enhanced* as com-
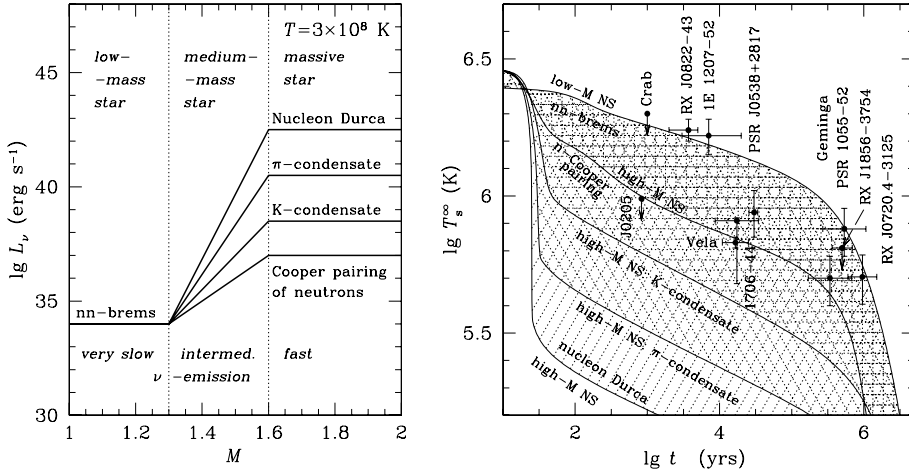
Figure 6. *Left:* A sketch of the neutrino luminosity L_ν versus stellar mass for NSs with the internal temperature $T = 3 \times 10^8$ K at four models of NS structure. *Right:* Four hatched regions of T_s^∞ which can be explained by cooling of NSs of different masses for four models in the left panel.

pared to the emission provided by the modified Urca process. An enhanced emission would lead to *fast* cooling, allowing one to explain the observations of NSs coldest for their ages. There are different enhancement levels for different models of NS internal structure. Four scenarios are presented in Fig. 6. The left panel is a rough sketch of the neutrino luminosity as a function of M at $T = 3 \times 10^8$ K. One can generally assume a slow neutrino emission in low-mass NSs (e.g., provided by the neutrino bremsstrahlung in neutron-neutron collisions), an enhanced neutrino emission in high-mass NSs, and the transition from the slow to enhanced emission with increasing M in medium-mass NSs. The mass range of medium-mass stars is model dependent [20]. In massive NSs L_ν scales as T^6 for all scenarios except for Cooper pairing scenario (where $L_\nu \propto T^8$ [4,3]). In low-mass NSs, $L_\nu \propto T^8$.

The right panel of Fig. 6 shows the limiting cooling curves for each scenario (no accreted envelopes). The upper curve refers to low-mass NSs. Their cooling is the same for all scenarios, and it explains the observations of NSs hottest for their age (Sect. 3.1). Four lower curves show cooling of maximum-mass NSs for four scenarios. They are the lowest cooling curves in these scenarios. The three lowest curves are taken from Ref. [2], while the fourth is from Ref. [4]. The range of T_s^∞ between the upper curve and a lower curve can be filled by cooling curves of NSs with masses from $\sim M_\odot$ to M_{max}. Thus, we have four different ranges of T_s^∞ (four hatched regions) for four scenarios.

The highest enhancement of neutrino emission is provided by the direct Urca (Durca) process in nucleon (or nucleon-hyperon) cores [21]. This scenario predicts the coldest mas-
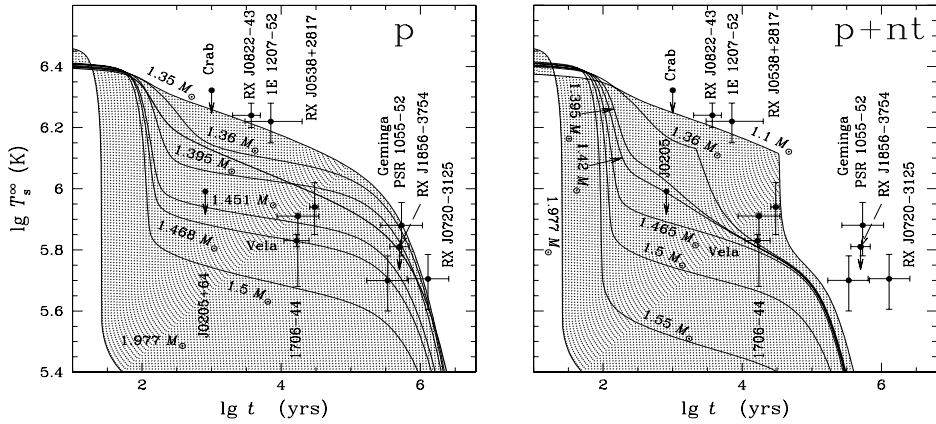
Figure 7. *Left:* Cooling of NSs of several masses (indicated near the curves). NSs are assumed to have nucleon cores and proton superfluidity p from Fig. 3. *Right:* Same as in the left panel but adding the effect of neutron superfluidity nt.

sive NSs and the widest theoretical T_s^∞ range. If the direct Urca process is forbidden but pion condensate is present in the inner NS core, the enhancement of neutrino emission is provided by the process of Durca type involving quasi-nucleons (e.g., [22]). This enhancement is weaker, the massive stars are hotter, and the acceptable T_s^∞ range narrower. If pion condensate is absent, but kaon condensate available, the neutrino emission enhancement (in Durca-type processes involving quasi-baryons [22]) is even weaker and the T_s^∞ range narrower. Nearly the same enhancement is expected in NSs with non-superfluid inner cores composed of quarks. Finally, the lowest enhancement can be produced in nucleon inner cores [3,4], where the direct Urca process is forbidden but mild superfluidity (e.g., of neutrons) is available (see Sect. 3.4). It triggers the Cooper pairing neutrino emission which accelerates NS cooling. It gives the narrowest theoretical region of T_s^∞.

As seen from Fig. 6, all four scenarios are compatible with the observations.

3.3. Cooling of medium-mass neutron stars

The next question, crucial for explaining the observations (e.g., of the Vela and Geminga pulsars), is how cooling curves fill hatched regions in Fig. 6 if we vary the NS mass from $\sim M_\odot$ to $M_{\max}$. The answer [23] is closely related to the contrast of slow and enhanced neutrino luminosities and the mass range of medium-mass NSs in Fig. 6. Let us outline this problem for NSs with nucleon cores.

Figure 7 shows cooling of NSs of several masses with the same EOS as in Fig. 3 (no accretion envelopes). In the left panel we take into account strong proton pairing p, which extends to densities $\rho > \rho_D$. As long as $T_{cp}(\rho) \gtrsim 3 \times 10^9$ K, it suppresses the modified and even the direct Urca process and leads to very slow neutrino emission. At higher ρ it gradually dies out, opening the direct Urca process. The gradual opening broadens the
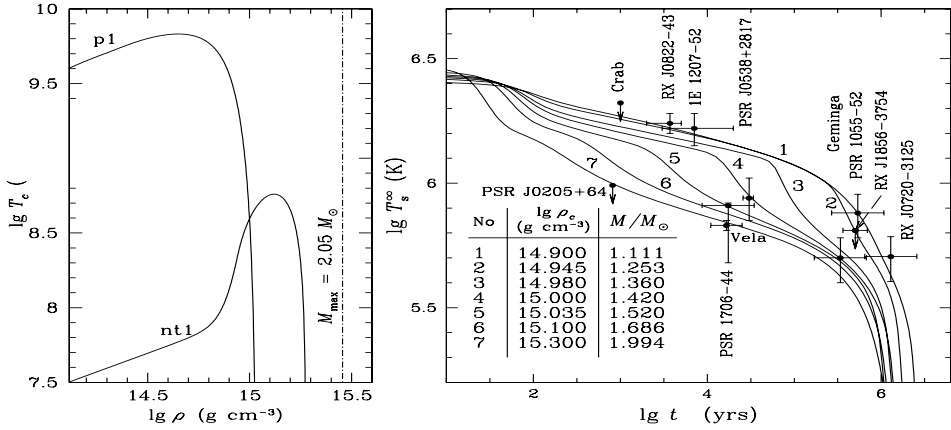
Figure 8. *Left:* Model density dependence of critical temperatures of protons (p1) and neutrons (nt1) in a nucleon NS core for the EOS which forbids the direct Urca process. *Right:* Cooling curves of NSs of several masses for the same EOS, taking into account superfluidities p1 and nt1. After Ref. [4].

direct Urca threshold (Fig. 3) and ensures the gradual decrease of cooling curves with increasing M. In this way we may attribute masses to observed NSs [24]. For instance, we obtain $M \approx 1.47 \, M_\odot$ for the Vela pulsar. However, this *weighing* of NSs is sensitive to the EOS of dense matter, the threshold of the direct Urca process, and the superfluidity model $T_{\rm cp}(\rho)$. Were superfluidity absent, the transition from slow to fast cooling would occur in a very narrow mass interval $(0 < M - M_{\rm D} \lesssim 0.001 \, M_\odot)$, and the successful interpretation of the data would be unlikely (e.g., Ref. [2]).

3.4. Harmful and useful Cooper-pairing neutrino emission

The cooling effect of neutrino emission due to Cooper pairing of nucleons may be different. For instance, let us assume the presence of neutron pairing nt with the peak of $T_{\rm cnt}(\rho)$ as low as $\sim 4 \times 10^8$ K at $\rho \sim 4 \times 10^{14}$ g cm^{-3} (Fig. 3). This superfluidity is mild and insignificant, according to nuclear physics standards, but crucial for NS cooling. It appears in a cooling star when the internal temperature falls below the peak value. It creates then a powerful neutrino emission owing to Cooper pairing of neutrons in outer NS cores (especially efficient in low-mass NSs). The emission accelerates NS cooling, as shown in the right panel of Fig. 7, and violates the interpretation of the observations of such sources as PSR B1055−52. Thus, this mild neutron superfluidity contradicts the observations.

The opposite example is given in Fig. 8. Let us consider NSs with nucleon cores and employ the EOS [25] which forbids the direct Urca process in all NSs with $M \leq M_{\rm max} = 2.05 \, M_\odot$. Furthermore, let us adopt the model of strong proton pairing p1 and mild neutron pairing nt1 (the left panel of Fig. 8). Pairing p1 is similar to pairing p in Fig.

3; it suppresses the modified Urca process in low-mass NSs. The peak of T_cnt pairing nt1 is as low as for pairing nt but shifted to higher densities. Accordingly, pairing nt1 is inefficient in low-mass stars and does not speed up their cooling. However, the enhanced neutrino emission owing to this pairing operates in massive NSs and accelerates their cooling (a scenario considered in Sect. 3.2, Fig. 6). Then, as seen in the right panel of Fig. 8, the cooling of NSs of different masses enables us to explain the data. In this case mild neutron pairing is useful for interpretation of the observations but a successful interpretation is possible only under stringent constraints on the $T_\mathrm{cnt}(\rho)$ profile [4]. Moreover, a discovery of a new NS slightly colder than those observed now would ruin this interpretation.

4. CONCLUSIONS

We have outlined several possible scenarios of NS cooling. In particular, we have considered cooling of NSs with nucleon (nucleon/hyperon) cores, and cores containing exotic phases of dense matter. We have shown that many scenarios are currently compatible with observations of thermal radiation from isolated NSs. Our main conclusions are:

(i) Some NSs (e.g., RX J0822−43 or PSR B1055−52) are hotter and some (e.g., the Vela pulsar) colder than non-superfluid NSs which cool via the modified Urca process. Hotter NSs are possibly low-mass stars, while coldest observed NSs are possibly more massive.

(ii) Currently, the observations unable one to discriminate between many cooling scenarios. However, they seem to rule out mild superfluidity with the peak of the critical temperature $T_\mathrm{c}(\rho)$ between $\sim 3 \times 10^8$ and $\sim 2 \times 10^9$ K at $\rho \lesssim 8 \times 10^{14}$ g cm^{-3} in NS cores. This superfluidity would initiate Cooper pairing neutrino emission in low-mass NSs hampering the interpretation of the observations of old and warm NSs, such as PSR B1055−52. In contrast, mild superfluidity with the peak of $T_\mathrm{c}(\rho)$ at *higher* ρ can be useful for interpretation of the observations.

We have discussed main cooling scenarios but not all of them. Some others are reviewed in Refs. [2,3]. Actually, the effects of superfluidity are more sophisticated than discussed above. For instance, cooling curves do not change qualitatively by exchanging $T_\mathrm{c}(\rho)$ for neutrons and protons [26]. Strong superfluidity of all baryon species (with peaks of $T_\mathrm{c}(\rho)$ higher than 2×10^9 K) leads to a very low heat capacity of NSs. Such stars appear at the photon cooling stage earlier than at $t \sim 10^5$ years; they are too cold at that stage. Weak superfluidity, with $T_\mathrm{c}(\rho) \lesssim 3 \times 10^8$ K, does not occur in NSs of ages $t \lesssim 10^5$ years and does not affect their cooling. Cooling of low-mass NSs can be strongly affected by singlet-state pairing of neutrons in inner stellar crusts.

New observations of NSs are required for a better understanding of their internal structure. New discoveries of cold NSs would be especially useful. Observations of cooling NSs can be analyzed together with other observational data, for instance, with observations of quiescent thermal emission from NSs in soft X-ray transients (see [2], for references). This would allow one to obtain more stringent constraints on NS structure.

55-2397).

REFERENCES

1. P. Haensel, In: Final Stages of Stellar Evolution, C. Motch and J.-M. Hameury (eds.), EAS Publications Series: EDP Sciences (2003) 249.
2. D.G. Yakovlev and C.J. Pethick, Ann. Rev. Astron. Astrophys. 42 (2004) 169.
3. D. Page, J.M. Lattimer, M. Prakash, and A.W. Steiner , Astroph. J. (2004) submitted [astro-ph/0403657].
4. M.E. Gusakov, A.D. Kaminker, D.G. Yakovlev, and O.Y. Gnedin, Astron. Astrophys. 423 (2004) 1063.
5. P. Slane, D.J. Helfand, E. van der Swaluw, and S.S. Murray, Astrophys. J. (2004) submitted [astro-ph/0405380].
6. M.C. Weisskopf, S.L. O'Dell, F. Paerels, R.F. Elsner, W. Becker, A.F. Tennant, and D.A. Swartz, Astrophys. J. 601 (2004) 1050.
7. V.E. Zavlin, J. Trümper, and G.G. Pavlov, Astrophys. J. 525 (1999) 959.
8. V.E. Zavlin, G.G. Pavlov, and D. Sanwal, Astrophys. J. 606 (2004) 444.
9. G.G. Pavlov, V.E. Zavlin, D. Sanwal, V. Burwitz, and G.P. Garmire, Astrophys. J. 552 (2001) L129.
10. K.E. McGowan, S. Zane, M. Cropper, J.A. Kennea, F.A. Córdova, C. Ho, T. Sasseen, and W.T. Vestrand. 2004. Astrophys. J. 600 (2004) 343.
11. V.E. Zavlin and G.G. Pavlov, Mem. Soc. Astron. Ital. (2004) in press [astro-ph/0312326].
12. G.G. Pavlov and V.E. Zavlin VE, In: Texas in Tuscany. XXI Texas Symposium on Relativistic Astrophysics, R. Bandiera, R. Maiolino, and F. Mannucci (eds), 319 (Singapore: World Scientific Publishing) 2003.
13. C. Motch, V.E. Zavlin, and F. Haberl, Astron. Astrophys. 408 (2003) 323.
14. O.Y. Gnedin, D.G. Yakovlev, and A.Y. Potekhin, MNRAS 324 (2001) 725.
15. A.Y. Potekhin, D.G. Yakovlev, G. Chabrier, and O.Y. Gnedin, Astrophys. J. 594 (2003) 404.
16. M. Prakash, T.L. Ainsworth, and J.M. Lattimer, Phys. Rev. Lett. 61 (1988) 2518.
17. U. Lombardo and H.-J. Schulze, In: Physics of Neutron Star Interiors, D. Blaschke, N.K. Glendenning, and A. Sedrakian (eds.), 30 (Springer: Berlin) 2001.
18. E.G. Flowers, M. Ruderman, and P.G. Sutherland, Astrophys. J. 205 (1976) 541.
19. P. Chang and L. Bildsten, Astrophys. J. 585 (2003) 464.
20. A.D. Kaminker, D.G. Yakovlev, and O.Y. Gnedin, Astron. Astrophys. 383 (2002) 1076.
21. J.M. Lattimer, C.J. Pethick, M. Prakash, and P. Haensel, Phys. Rev. Lett. 66 (1991) 2701.
22. C.J. Pethick, Rev. Mod. Phys. 64 (1992) 1133.
23. D.G. Yakovlev and P. Haensel, Astron. Astrophys. 407 (2003) 259.
24. A.D. Kaminker, P. Haensel, and D.G. Yakovlev, Astron. Astrophys. 373 (2001) L17.
25. F. Douchin and P. Haensel, Astron. Astrophys. 380 (2001) 151.
26. M.E. Gusakov, A.D. Kaminker, D.G. Yakovlev, and O.Y. Gnedin, Astron. Lett. 30 (2004) 758